J. Biochem. **144,** 121–130 (2008)
doi:10.1093/jb/mvn049

Direct Observation of Conformational Folding Coupled with Disulphide Rearrangement by Using a Water-soluble Selenoxide Reagent—A Case of Oxidative Regeneration of Ribonuclease A under Weakly Basic Conditions

Michio Iwaoka[1],*, Fumio Kumakura[1], Mitsumasa Yoneda[1], Toshitaka Nakahara[1], Kayo Henmi[1], Hiromi Aonuma[1], Hiroyasu Nakatani[2] and Shuji Tomoda[2]

[1]Department of Chemistry, School of Science, Tokai University, Kitakaname, Hiratsuka-shi, Kanagawa 259-1292; and [2]Department of Life Sciences, Graduate School of Arts and Sciences, The University of Tokyo, Komaba, Meguro-ku, Tokyo 153-8902, Japan

Received March 8, 2008; accepted April 8, 2008; published online April 11, 2008

Oxidative regeneration pathways of bovine pancreatic ribonuclease A (RNase A), which has four SS linkages, were studied at 25°C and pH 8.0 by using *trans*-3, 4-dihydroxy-1-selenolane oxide (DHS^{ox}), a new selenoxide reagent with strong oxidation power. The short-term folding study using a quench-flow instrument (~1 min) revealed that early intermediates (1S, 2S, 3S and 4S) are formed stochastically and irreversibly from the reduced protein (R) and do not have any stable structures. In the long-term folding study (~300 min), on the other hand, slow generation of the key intermediates (des[65–72] and des[40–95]) through SS rearrangement from the 3S intermediate ensemble was observed, followed by slight formation of native RNase A (N). The parallel UV and CD measurements demonstrated that formation of the key intermediates is accompanied with the formation of the native-like structures. Thus, DHS^{ox} allowed facile identification of the conformational folding steps coupled with SS rearrangement on the major oxidative folding pathways.

Key words: CD, disulphide, protein folding, selenium, UV.

Abbreviations: 1S, 2S, 3S and 4S, ensembles of folding intermediates of RNase A with one, two, three and four SS linkages, respectively; AEMTS, 2-aminoethyl methanethiosulphonate; des[40–95], a folding intermediate of RNase A having three native SS linkages and lacking the Cys40–Cys95 SS linkage; des[65–72], a folding intermediate of RNase A having three native SS linkages and lacking the Cys65–Cys72 SS linkage; DHS^{ox}, DL-trans-3,4-dihydroxy-1-selenolane oxide; DHS^{red}, DL-*trans*-3,4-dihydroxy-1-selenolane; DTT^{ox}, *trans*-4,5-dihydroxy-1,2-dithiane (oxidized dithiothreitol); DTT^{red}, DL-dithiothreitol; N, the folded state of RNase A with four native SS linkages; R, a fully reduced state of RNase A; RNase A, bovine pancreatic ribonuclease A; SH, thiol; SS, disulphide.

Oxidative folding of a protein with several disulphide (SS) linkages has attracted large interest of biological chemists since the landmark study of Anfinsen (*1*). However, regeneration processes of the native SS linkages from the reduced form of a protein suffer from significant complications due to formation of a large number of the partially oxidized intermediates; hence it is not an easy task to identify the major folding pathway(s) and characterize the key intermediates (*2–6*). We present here that the task can be achieved simply by using a new selenium oxidant, DL-trans-3,4-dihydroxy-1-selenolane oxide (DHS^{ox}) (*7*, *8*), as demonstrated for the case of oxidative refolding of bovine pancreatic ribonuclease A (RNase A) (*9*, *10*).

Recovery of the native structures (*i.e.* regeneration of the native SS linkages) from a reduced protein requires two fundamental processes; SS formation and SS rearrangement (or SS reshuffling) reactions (*11*). The former corresponds to the oxidation of two cysteinyl thiol (SH) groups to produce a SS bond, and the latter does to the intramolecular exchange of a SS bond by using free SH groups. The SS rearrangement is an indispensable process to obtain the native SS linkages because the SS formation should not necessarily occur between a correct pair of the cysteine residues.

Various oxidation conditions have been applied to the study of the oxidative folding pathways of SS-containing proteins (*2–6*). The most widely used redox couples are glutathione (GSSG/GSH) and dithiothreitol [*trans*-4, 5-dihydroxy-1,2-dithiane (oxidized dithiothreitol) (DTT^{ox})/DL-dithiothreitol (DTT^{red})]. These sulphur-containing reagents react with a reduced and denatured protein to generate a variety of partially oxidized intermediates and then reproduce the native form gradually from the complex mixture of the intermediates through SS formation as well as SS rearrangement reactions: DTT^{ox} has more advantages as an oxidant than GSSG does because it does not form the stable mixed-SS species with a protein (*12*, *13*). Although oxidative folding pathways have been well deduced for some model proteins, such as BPTI (*14–16*), RNase A (*11–13*, *17–19*), lysozyme (*20–26*), α-lactalbumin (*27–29*), by using the sulphur reagents,

*To whom correspondence should be addressed. Tel: +81-463-58-1211, Fax: +81-463-50-2094, E-mail: miwaoka@tokai.ac.jp

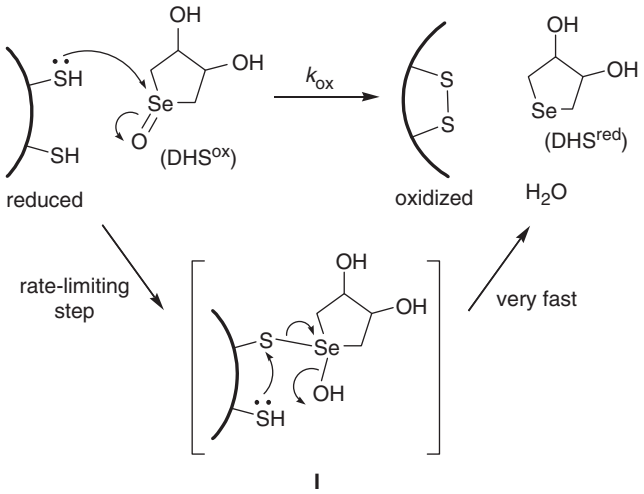

Fig. 1. **The reaction scheme and the plausible mechanism for SS-bond formation by DHS^{ox} in a reduced protein.** Species I is an unstable intermediate having an S–Se linkage between the protein and DHS.

it is still difficult to characterize the key intermediates, which appear along the major oxidative folding pathways, directly under the normally applied regeneration conditions.

Recently, new types of oxidative folding reagents have been tested, including polymer-bound sulphur-containing reagents (*30*) and platinum complexes (*31–33*). Protein SS isomerase (*34*, *35*) and its active-site model (*36*) have also been used for the study of oxidative protein folding. Selenoglutathione, a selenium analogue of GSSG, would be another useful reagent for oxidation of protein SH groups (*37*). However, none of these reagents has successfully been applied to characterization of the key intermediates. It is also important to notice that the rate-limiting step on the major folding pathways of a protein could change from one to another depending on the applied oxidation conditions.

We recently synthesized a new oxidant, DHS^{ox} (*7*, *8*), which contains a selenium atom as the reaction centre in a form of selenoxide. When DHS^{ox} was applied to oxidative regeneration of RNase A, which has four SS linkages (Cys26–Cys84, Cys40–Cys95, Cys58–Cys110 and Cys65–Cys72), the SS formation proceeded very fast (<1 min) and quantitatively in a wide range of pH (pH 3–9) (*7*). The reaction mechanism for the oxidation with a reduced protein is shown in Fig. 1. The reaction would take place in two steps; the selenoxide is attacked by a protein SH group to form unstable intermediate I having a S–Se linkage, which is rapidly cleaved by a subsequent intramolecular attack by the second SH group to form reduced DHS [DL-*trans*-3,4-dihydroxy-1-selenolane (DHS^{red})] leaving a SS linkage in the protein. The second step would proceed very fast and quantitatively, so the intermediate I would not be significantly populated during the oxidation reaction of a reduced protein. This means that the rate-limiting step is the first bimolecular step and the apparent reaction rate of the SS formation (k_{ox}) should be controlled by the

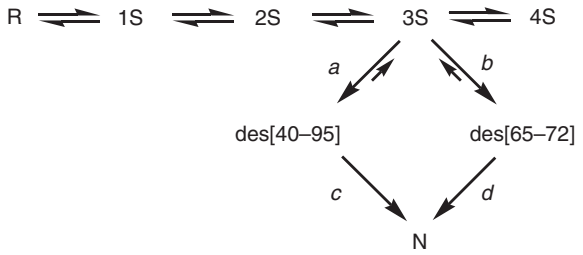

Fig. 2. **SS-coupled folding pathways of RNase A.** Processes *a* and *b* are SS rearrangement steps accompanied with formation of the native-like structures. Processes *c* and *d* are final folding steps to the native state (N) with the formation of native Cys40–Cys95 and Cys65–Cys72 SS linkages, respectively.

probability of DHS^{ox} to meet the SH groups of a protein molecule.

The major oxidative regeneration pathways of RNase A have been elaborately established as shown in Fig. 2 (*18*). R, 1S, 2S, 3S and 4S intermediates attain a pre-equilibrium with a redox couple, and the conformational folding steps are the SS rearrangement from 3S to des[40–95] and des[65–72] intermediates (*i.e*. processes *a* and *b*, respectively), which are subsequently oxidized to N through processes *c* and *d*. Therefore, of particular interest from a view point of the conformational folding of RNase A is to elucidate the detailed events that occur at processes *a* and *b*. Under regeneration conditions by using an excess amount of DTT^{ox}, however, the two key intermediates, *i.e*. des[40–95] and des[65–72], were difficult to be characterized because their populations were quite low due to the rapid oxidation to N, while their existence on the folding pathways could be evidenced by applying the reduction-pulse method (*19*, *38*).

In this article, we reinvestigated the oxidative regeneration pathways of RNase A (Fig. 2) by applying DHS^{ox} and found that this unique strong oxidant is potentially useful for direct observation of the conformational folding coupled with the SS rearrangement under slightly basic conditions. Two types of folding experiments were carried out. One is called the *short-term folding* study, in which the early kinetics of RNase A folding was analysed by using a quench flow instrument (Fig. 3). The other is called the *long-term folding* study, in which evolution of the native structures coupled with the slow SS rearrangement reaction was investigated. These two experiments are essentially same with each other in that the oxidation reaction was initiated just by mixing the solutions of reduced RNase A (R) and DHS^{ox}, except for a range of the reaction time. Throughout the article, we distinguishingly used the two terms, 'SS rearrangement' and 'SS reshuffling', so that the former is for the slow intramolecular process of the SS intermediates to form a specific SS intermediate with a stable structure, whereas the latter is for the fast random intramolecular process to exchange the SS linkages without formation of a stable structure.

MATERIALS AND METHODS

Materials—RNase A (type 1-A) was purchased from Sigma–Aldrich Japan and used without further purification. DHS^{ox} (*8*) and 2-aminoethyl methanethiosulphonate

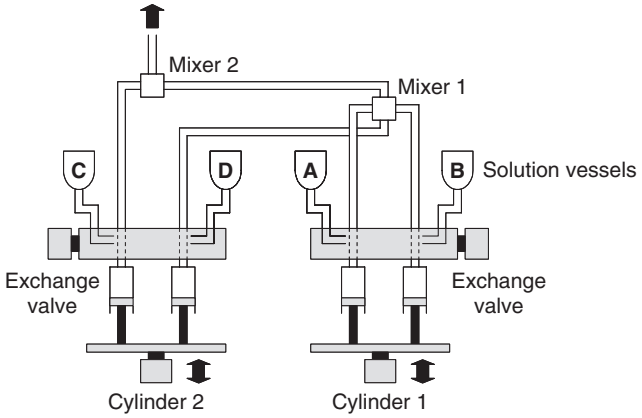

Fig. 3. **A quench-flow instrument used for the short-term folding experiment.** Reduced RNase A (R), DHS^{ox}, AEMTS and Tris–HCl/1 mM EDTA buffer solutions at pH 8.0 were loaded in vessels A, B, C and D, respectively. When cylinder 1 is moved up, the oxidation of R with DHS^{ox} starts and the reaction mixture remains in the tube between mixers 1 and 2. After a certain time, cylinder 2 is moved up and AEMTS quenches the oxidation reaction. The whole system was maintained at 25.0 ± 0.1°C.

(AEMTS) (*39*) were synthesized according to the literature methods. All other reagents were commercially available and used without further purification.

Preparation of Reduced RNase A (R)—The experimental procedure described in the literature (*12*) was followed with slight modification. To a solution of RNase A (5–10 mg) dissolved in 0.5 ml of a 100 mM Tris–HCl/1 mM EDTA buffer solution at pH 8.0 containing 4 M guanidine thiocyanate as a denaturant was added an excess amount of DTT^{red} (7–12 mg). After standing at room temperature for 40 min, the reaction mixture was passed through Sephadex G25 resin that had been equilibrated with a 100 mM Tris–HCl/1 mM EDTA buffer solution at pH 8.0 purged with nitrogen. The concentration of the reduced RNase A (R) desalted in the Tris buffer solution was determined by UV absorbance at 275 nm ($\varepsilon = 8{,}600\ M^{-1}\,cm^{-1}$) (*12*). The R solution was immediately used in the two types of folding experiments described subsequently.

Short-term Folding Experiment—A quench-flow instrument (a Unisoku quench-mixer equipped with a mixer controller unit, Fig. 3) was set up by loading the obtained R solution, a DHS^{ox} solution in 100 mM Tris–HCl/1 mM EDTA at pH 8.0, an AEMTS solution in 100 mM Tris–HCl/1 mM EDTA at pH 8.0 and a drive solution (a 100 mM Tris–HCl/1 mM EDTA solution at pH 8.0) in vessels A, B, C and D, respectively. The concentration of DHS^{ox} was regulated to be 1–6 M ratios with respect to the reduced protein (R), and the concentration of AEMTS was regulated to be >100 M ratios with respect to R. The whole instrument was maintained at 25.0 ± 0.1°C by a thermostatted water bath system. Fifty microlitre each of solutions A and B were mixed rapidly and held between mixers 1 and 2 after the first push (cylinder 1), while on the second push (cylinder 2) 109 μl each of solution C and solution D were simultaneously injected, and 218 μl of the quenched solution was squeezed out from a drain tube of mixer 2. The SS formation reaction was initiated by the first push and was quenched by AEMTS (a SH-blocking reagent) on the second push. The reaction time, *i.e.* a time lag between the first and second pushes, was changed from 50 ms to 60 s. The collected sample solutions were acidified by addition of 2 μl of acetic acid and stored in a freezer at −30°C until the samples were analysed by HPLC.

Long-term Folding Experiment—A DHS^{ox} solution in 100 mM Tris–HCl/1 mM EDTA at pH 8.0 was prepared so that the concentration of DHS^{ox} was 1–4 times higher than that of the reduced RNase A (R). To 200 μl of the DHS^{ox} solution was manually added 200 μl of the R solution in a 1.5 ml micro test tube all at once, and the mixture was stirred for 10 s. After standing for a certain period of time (1–300 min) in a dry thermo bath regulated at 25.0 ± 0.1°C, 200 μl of a 100 mM Tris–HCl/1 mM EDTA solution at pH 8.0 containing AEMTS (~7 mg/ml) was added to the resulting solution to quench the SS reshuffling and rearrangement reactions. The same folding experiments were also carried out in a globe box filled with an argon gas (>99.999%) to check the effects of air oxidation on the relative populations of the generated folding intermediates. The collected sample solutions were acidified with acetic acid and stored in a freezer at –30°C.

To investigate evolution of the native-like structures during the long-term folding experiment, the UV and CD spectra were measured on a Shimadzu UV-1700 spectrophotometer and a Jasco J-820 spectropolarimeter, respectively, in parallel to the above manual quenching experiment. For the UV measurement, 500 μl each of the desalted R solution and the DHS^{ox} solution were mixed and poured into a 1 ml quartz cell, which was set in the UV cell holder thermostatted at 25.0 ± 0.1°C. For the CD measurement, 150 μl of the desalted R solution was diluted with 900 μl of H_2O in a 1.5 ml micro test tube and then added with 150 μl of the DHS^{ox} solution. The mixture was poured into a 1 ml quartz cell, which was set in the CD cell holder thermostatted at 25.0 ± 0.1°C. The pH of the DHS^{ox} solution was kept constant at 8.0 ± 0.1 during the dilution process with H_2O.

HPLC Analysis—A Shimadzu VP series high performance liquid chromatograph system equipped with a 5 ml sample loop and a Tosoh TSKgel SP-5WP strong cation exchange column (7.5 × 75 mm) was used. The sample solutions with different reaction times, each of which contained the same amount of the protein (0.1–0.2 mg, depending on the initial concentration), were thawed and desalted into a 0.1 M acetic acid solution through a Sephadex G25 column before injection to the HPLC system, which had been equilibrated with a 25 mM HEPES/1 mM EDTA solution at pH 7.0 (buffer A) at the flow rate of 0.5 ml/min. After sample injection, a gradient of sodium sulphate (Na_2SO_4) was applied by changing the ratio of buffer B (buffer A + 0.5 M Na_2SO_4) from 0% to 45% in 50 min. A wavelength of the UV detector was set to 280 nm. The recorded signals were integrated and analysed by using a Shimadzu LCsolution software. The injected protein was quantitatively eluted through the column as checked by the total integral areas of the signals on the chromatograms.

MS Analysis—A Jeol JMS-T100LP mass spectrometer connected to an Agilent 1200 series HPLC system was

used for the measurement of a high-resolution mass spectrum for each intermediate separated by the cation exchange column. The fractionated intermediates were collected, desalted in 0.1 M acetic acid and lyophilized. The samples (~0.1 mg) were dissolved in 100 µl of 100 mM Tris–HCl/1 mM EDTA at pH 8.0 and directly infused to the chamber of the mass spectrometer under electron spray ionization conditions. Angiotensin was used as a standard. To identify the SS linkages present in the des[40–95] and des[65–72] intermediates, the procedure reported in the literature (*40*) was followed. The lyophilized samples (~0.1 mg) were dissolved in 100 µl of 100 mM Tris–HCl/1 mM EDTA at pH 8.0 and digested at 25°C with trypsin for 1 h and then α-chymotrypsin for 1 h: 1 µl each of trypsin and α-chymotrypsin dissolved in 1 mM HCl (1.5 mg/ml) were added to the sample solutions in the sequence. The resulting solutions were injected to the LC unit of the mass spectrometer equipped with a Tosoh TSKgel Octadecyl-4PW column (2.0 × 150 mm). A binary solution gradient (A: B = 98: 2–55: 45 in 50 min; A, 0.09% TFA in H_2O; B, 0.09% TFA in CH_3CN) was applied with the flow rate of 0.1 ml/min.

RESULTS AND DISCUSSION

Short-term Folding of RNase A Using DHS^{ox}—Oxidation of completely reduced RNase A (R), which has eight cysteinyl SH groups along the peptide chain, was carried out at 25°C and pH 8.0 by using a quench-flow instrument (Fig. 3), changing a reaction time (50 ms to 60 s) and a molar ratio of DHS^{ox} with respect to R (1–6 M equivalents). By reaction with AEMTS, the oxidation intermediates should gain 76 Da in the molecular mass and one positive charge per one SH group due to the modification to $SSCH_2CH_2NH_3^+$, hence the intermediates could be identified by mass spectroscopy (see the Supplementary Data) and separated into groups by HPLC using a cation exchange column at pH 7.0 (*12*), depending on the number of the remaining SH groups (or the number of the formed SS bridges). The pertinent HPLC charts with a reaction time of 10 s are shown in Fig. 4.

When R was added with 1 M equivalent of DHS^{ox}, 1S, which has one SS linkage, was formed as a main ensemble of the products in 10 s accompanied by a small amount of 2S, which has two SS linkages (Fig. 4A). These SS ensembles were mixtures of a number of intermediates with various types of SS linkages as deduced from the peak profiles. Similarly, 2S and 3S were formed as main products when R and DHS^{ox} were reacted in the 1 : 2 and 1 : 3 ratios, respectively (Figs 4B and C). 4S, which has four SS linkages but is not native RNase A (N), was dominantly observed when >4 M equivalents of DHS^{ox} were added to R (Fig. 4D). The results clearly demonstrated that DHS^{ox} reacts protein SH groups to form SS linkages quantitatively and rapidly. This is in sharp contrast to normally used sulphur-containing reagents, such as DTT^{ox} and GSSG: with these reagents the oxidation of cysteinyl SH groups requires a much longer reaction time (minutes to hours) even in the presence of excess amounts of the reagents (*12*). It should also be noted that the peak profiles for each SS ensemble

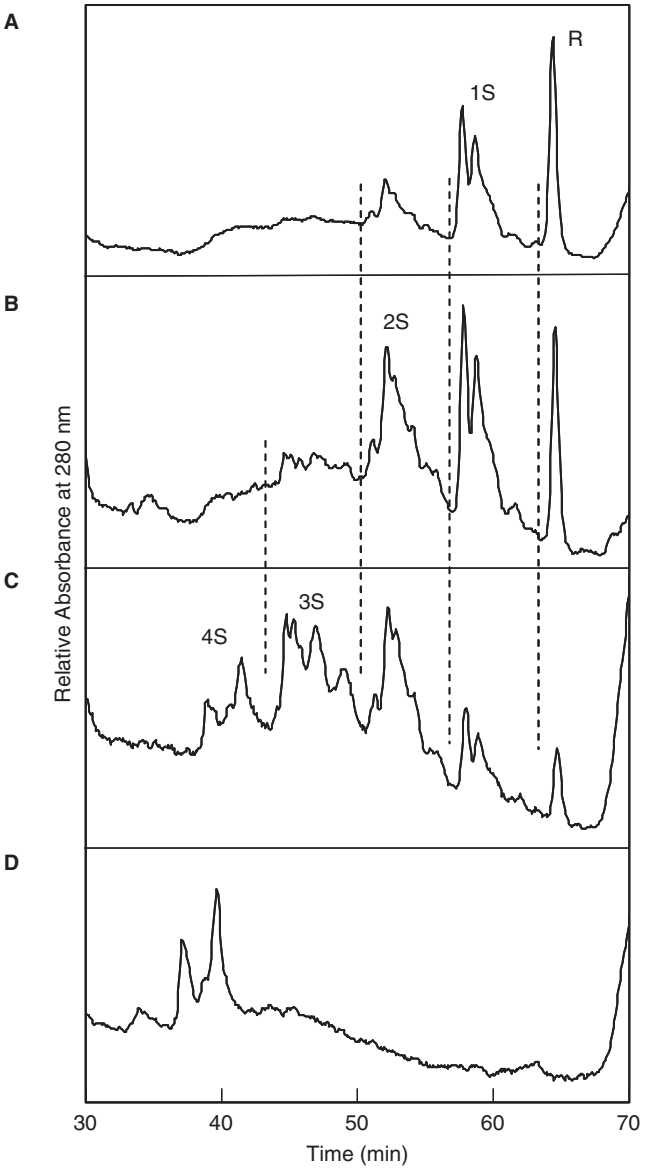

Fig. 4. **HPLC chromatograms obtained from the short-term folding experiments of RNase A using DHS^{ox} as an oxidizing reagent at 25.0°C and pH 8.0. The reaction time was 10 s.** (A) 1 equivalent of DHS^{ox} was reacted; $[R]_0 = [DHS^{ox}]_0 = 52.3$ µM. (B) 2 equivalents of DHS^{ox} were reacted; $[R]_0 = [DHS^{ox}]_0/2 = 27.0$ µM. (C) 3 equivalents of DHS^{ox} were reacted; $[R]_0 = [DHS^{ox}]_0/3 = 45.8$ µM. (D) 4 equivalents of DHS^{ox} were reacted; $[R]_0 = [DHS^{ox}]_0/4 = 31.3$ µM. See the text for details of the HPLC analysis conditions.

on the HPLC charts of Fig. 4 resembled those obtained from the folding experiments of RNase A using DTT^{ox} as an oxidizing reagent (see the Supplementary Data). The similarity suggested that the SS components of each SS ensemble do not change by using DHS^{ox} as an oxidizing reagent.

Kinetic Analysis—Figure 5 shows the changes of relative populations of the SS intermediates as a function of a reaction time (a logarithmic scale) when 3 M equivalents of DHS^{ox} were added to R. R was almost completely consumed in 10 s, and 1S, 2S, 3S and 4S were

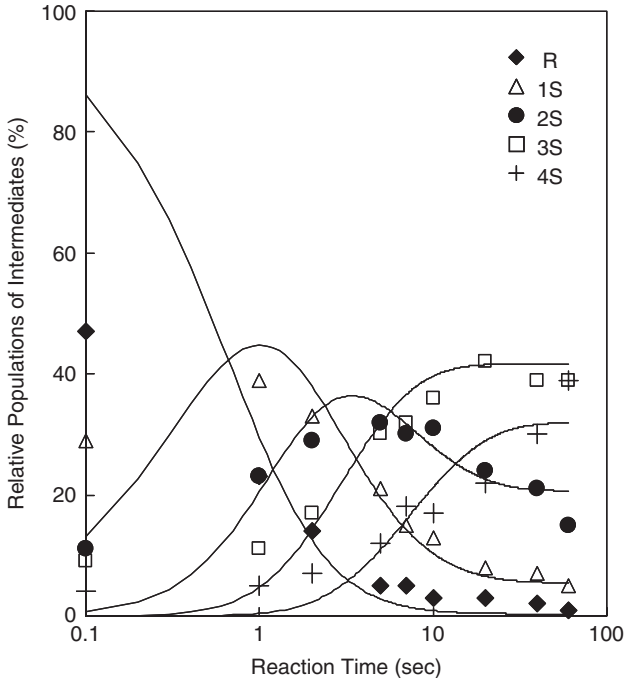

Fig. 5. **Relative populations of SS-folding intermediates as a function of the reaction time.** Reaction conditions were $[R]_0 = [DHS^{ox}]_0/3 = 16.5\,\mu M$ at 25.0°C and pH 8.0. Lines were drawn by the simulation using the second-order rate constants of $k_1 = 30.6$, $k_2 = 20.1$, $k_3 = 14.9$ and $k_4 = 7.4\,mM^{-1}\,s^{-1}$ based on the folding scheme of R → 1S → 2S → 3S → 4S (Eq. 1).

sequentially generated in the order. Since only 3 M equivalents of DHS^{ox} were used, the main product was 3S after 20 s. It is notable that the oxidation reaction was almost completed in ~40 s.

According to the results shown in Figs 4 and 5 and those obtained under other reaction conditions, the reaction scheme for oxidative folding of RNase A using DHS^{ox} as an oxidizing reagent was drawn as

$$\mathrm{R} \xrightarrow{DHS^{ox}\ DHS^{red}} 1S \xrightarrow{DHS^{ox}\ DHS^{red}} 2S \xrightarrow{DHS^{ox}\ DHS^{red}} 3S \xrightarrow{DHS^{ox}\ DHS^{red}} 4S \quad (1)$$

The reverse reactions would be negligible at least in a short term (<60 s) because of the following reasons. First, the oxidation reaction proceeded quantitatively (Fig. 4). Second, addition of a large amount of DHS^{red} to the reaction mixture of R and DHS^{ox} did not affect relative populations of the SS ensembles.

Based on the reaction scheme of Eq. 1, the time-dependent data of relative populations of the oxidative folding intermediates, which were obtained with a reaction time of 300 ms to 60 s under seven different conditions using 1–6 M equivalents of DHS^{ox}, were fitted to determine the four second-order rate constants (k_1–k_4; k_1 for R → 1S, k_2 for 1S → 2S, k_3 for 2S → 3S and k_4 for 3S → 4S). Considering peak overlapping between the SS ensembles on the HPLC charts (Fig. 4), we assumed a maximum of 10% experimental errors on the relative populations in the data fitting. The values obtained for k_1–k_4 were 30.6 ± 0.9, 20.1 ± 0.7, 14.9 ± 0.8 and $7.4 \pm 0.4\,mM^{-1}\,s^{-1}$, respectively. The simulation using these rate constants well reproduced the experimental data, except for those with the reaction time of <300 ms, as shown with solid lines in Fig. 5, supporting the reaction scheme of Eq. 1.

Accuracy of HPLC Data—There are two important factors that would affect the accuracy of HPLC data; peak overlapping between the SS ensembles and errors in the reaction time.

Ensembles of 1S, 2S, 3S and 4S intermediates appeared on the HPLC chromatograms with different retention times depending on the number of the remaining SH groups along the chain because the blocking with AEMTS appended one positive charge (*i.e.* $SCH_2CH_2NH_3^+$) per one SH group (*12*). However, the SS ensembles were not so sharply separated from each other due to the slight peak overlapping as seen in Fig. 4. Nevertheless, the effects of the peak overlapping on the relative populations of SS ensembles must be limited because the fitting results well reproduced the experimental data as seen in Fig. 5. Moreover, when the yields of SS conversion (%SS) were calculated from relative populations of the SS ensembles according to the equation, $\%SS = (\%1S) \times 1 + (\%2S) \times 2 + (\%3S) \times 3 + (\%4S) \times 4$, the obtained values reasonably increased up to 100–400% in 30 s depending on the ratio of DHS^{ox} added.

On the other hand, accuracy of the reaction time would depend on two factors; the reaction rate of AEMTS toward a free SH group and a dead mixing time of the quench-flow mixer. In the data fitting analysis, we found that the relative populations of SS ensembles obtained in a reaction time shorter than 300 ms were not well reproduced by the reaction scheme of Eq. 1; for example, see the data obtained in the reaction time of 100 ms shown in Fig. 5. Therefore, the error of the reaction time would be within 300 ms in the short-term folding experiment, which was quite small as compared with a range of the reaction time (~60 s). Both the quenching rate of AEMTS and the dead mixing time would contribute to the observed error of a reaction time. However, the latter may be more significant because the second-order rate constants for the reactions of methyl methanethiosulphonate with various aliphatic thiolate anions are $\sim 10^6\,M^{-1}\,s^{-1}$ (*41*), indicating that the SS formation reaction can be quenched with AEMTS in a time scale of <1 ms under the conditions where the pH was 8.0 and the concentration of AEMTS was ca. 10 mM.

To summarize the above considerations, the HPLC data have been obtained with sufficient accuracy for the following discussion.

Early Folding Events—The values of second-order rate constants k_1–k_4 were roughly in a ratio of 4 : 3 : 2 : 1. This suggested stochastic formation of the SS bridges in the early folding intermediates depending simply on the number of free SH groups remaining along the chain (Fig. 1).

By considering the statistical factors (*i.e.* the number of the SH groups present in each intermediate ensemble), the averaged second-order rate constant of SS formation with DHS^{ox} (k_{ox}) was estimated to be $7.3\,mM^{-1}\,s^{-1}$, which is almost seven orders of magnitude larger than the averaged rate constant with DTT^{ox} ($\sim 0.05\,M^{-1}\,min^{-1}$) (*19*). When DTT was used as a redox couple, different

statistical factors (*i.e*. 28 : 15 : 6 : 1) were applied to obtain the averaged value (*19*). The discrepancy would be reflected by the different reaction mechanisms for DTT^{ox} and DHS^{ox}: the rate-limiting step is the intramolecular step for DTT^{ox} while it is the first bimolecular step for DHS^{ox} as shown in the reaction scheme of Fig. 1.

The stochastic behaviour observed for the oxidation of Eq. 1 is in accord with the conclusion by Scheraga and coworkers (*18*, *19*) that stable structures that may prevent or accelerate the SS formation and SS reduction are not yet present in R, 1S, 2S, 3S and 4S intermediates. The CD and UV spectra that we obtained in the reaction time of 1 min also supported the absence of the native-like structures in the intermediates. Thus, the early events in the oxidative folding pathways of RNase A could be reconfirmed to be just stochastic formation of SS linkages without generation of stable structures.

In addition to the SS formation, the SS reshuffling reaction must take place in each SS ensemble except for 4S. The time constants of SS reshuffling for 1S, 2S and 3S intermediates of RNase A can be estimated to be ca. 0.5, 1 and 9 s, respectively, at 25°C and pH 8.0 by using the reported rate constants of the intramolecular SS formation (k_{intra}) (*19*). Therefore, SS reshuffling could compete with SS formation in the reaction mixture for the short-term folding experiments. This suggests the possibility that the relative populations of the individual intermediates among 1S, 2S or 3S ensemble change with increasing a reaction time. However, the line shapes of the HPLC charts obtained for each SS ensemble scarcely changed during the short-term folding experiments (300 ms to 60 s). The observation is consistent with the absence of stable structures in the early folding intermediates because the relative populations within the kinetically formed SS ensembles in the very early stage of the folding (~1 s) already reflected the relative thermodynamic stabilities at 25°C and pH 8.0 to a large extent.

Significantly dominant formation of a specific Cys65–Cys72 SS linkage was previously pointed out in the 1S and 2S ensembles by using DTT^{ox} as an oxidative folding reagent (*40*, *42*). Since the line shapes of the HPLC chromatograms for 1S and 2S ensembles observed in the oxidative folding experiments using DTT^{ox} (see the Supplementary Data) were similar to those observed in the short-term folding experiments using DHS^{ox} (Fig. 4), it was strongly suggested that the same SS linkage can form dominantly within 1 s in the 1S and 2S intermediates.

Long-term Folding of RNase A Using DHS^{ox}—After the short-term folding events were over, there remained a mixture of various folding intermediates of RNase A (*i.e*. R, 1S, 2S, 3S and 4S) and DHS^{red} in the reaction solution. For example, when 3 M equivalents of DHS^{ox} were used, there were 3S as a major intermediate ensemble and 2S and 4S as minor ones with slight amounts of R and 1S after 1 min (Fig. 5). The reaction seemed to have been already completed. However, this is not correct as 1S, 2S and 3S intermediates still have free cysteinyl SH groups that can react with SS bonds to exchange the SS linkages. Therefore, we investigated the reaction intermediates that formed in a prolonged reaction time after the early folding events ended.

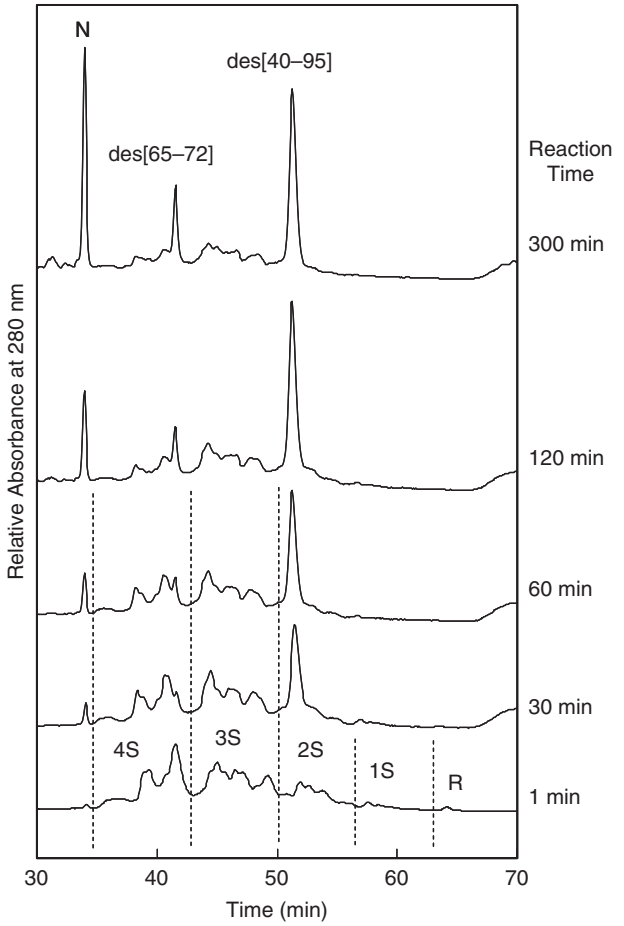

Fig. 6. **HPLC chromatograms obtained from the long-term folding experiment of RNase A using DHS^{ox} as an oxidizing reagent.** Reaction conditions were $[R]_0 = [DHS^{ox}]_0/3 = 18.3\ \mu M$ at 25.0°C and pH 8.0. See the text for details of the HPLC analysis conditions.

When 3 M equivalents of DHS^{ox} were reacted with R, growing of three distinct peaks was observed in the HPLC charts until the reaction time was ~300 min (Fig. 6). These peaks were unambiguously assigned to native RNase A (N) and des[65–72] and des[40–95] intermediates by comparison with the authentic reference sample and LC–MS analysis of the samples digested with trypsin and α-chymotrypsin. The assignments were consistent with the HPLC data reported in the literature (*18*). The peak growths were no longer observed after 300 min. When 1, 2 or 4 M equivalents of DHS^{ox} were reacted with R, such obvious changes as Fig. 6 were not observed in the HPLC charts within the reaction time of 300 min: slight formation of des[65–72], des[40–95] and N was detected only when 2 equivalents of DHS^{ox} were reacted.

With promotion of the SS rearrangement to des[65–72] and des[40–95] (Fig. 6), obvious changes were also recorded in the UV and CD spectra (Figs 7 and 8, respectively). In the UV spectrum, the absorptions at 287 and 280 nm increased with an isosbestic point at 275 nm. The observed spectral changes were completely opposite to those detected in the SS-intact conformational

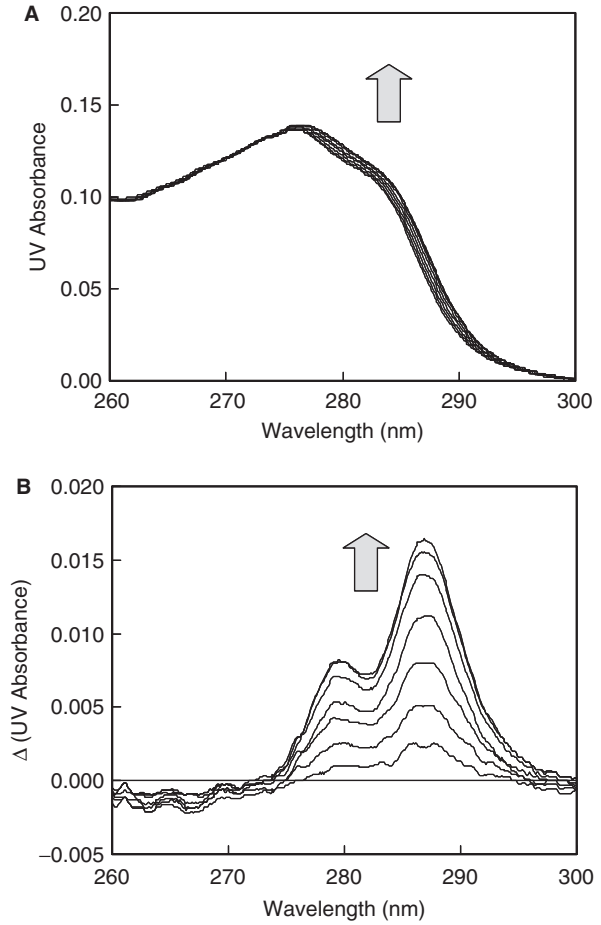

Fig. 7. **UV absorbance changes observed in the long-term folding experiment of RNase A using DHS^{ox} as an oxidizing reagent.** Reaction conditions were $[R]_0 = [DHS^{ox}]_0/3 = 14.7\,\mu M$ at 25.0°C and pH 8.0. (A) Superimposed UV spectra measured on 1, 15, 30, 60, 120, 180, 240 and 300 min after initiation of the reaction. (B) Differential UV spectra with respect to the UV spectrum obtained at the reaction time of 1 min.

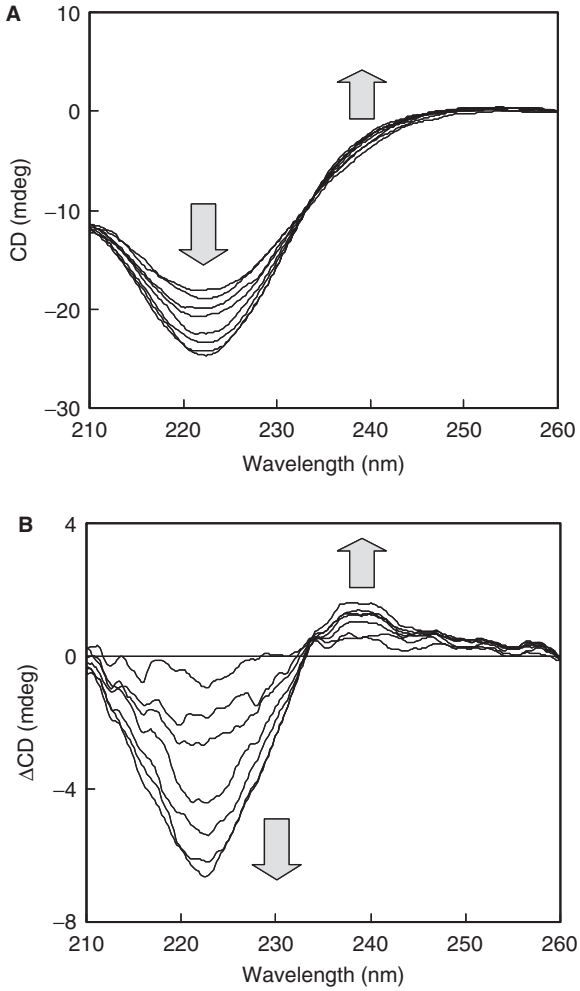

Fig. 8. **CD spectral changes observed in the long-term folding experiment of RNase A using DHS^{ox} as an oxidizing reagent.** Reaction conditions were $[R]_0 = [DHS^{ox}]_0/3 = 4.60\,\mu M$ at 25.0°C and pH 8.0. (A) Superimposed CD spectra measured on 1, 15, 30, 60, 120, 180, 240 and 300 min after initiation of the reaction. (B) Differential CD spectra with respect to the CD spectrum obtained at the reaction time of 1 min.

unfolding of RNase A in the heat denaturation experiment (*43*), although the intensity change was attenuated to about 60% of the expected range if the oxidative folding intermediates fully folded to N. The UV spectral change was not observed after 300 min. In the CD spectrum (Fig. 8), a negative signal grew at 222 nm, while a positive signal appeared at around 240 nm with an isosbestic point at 234 nm. The observed spectral changes were again opposite to those detected in the SS-intact conformational unfolding of RNase A in the heat denaturation (*44*).

Conformational Folding Events—The conformational folding steps in the oxidative folding pathways of RNase A have been assigned to the SS rearrangement processes from 3S to des[65–72] and des[40–95] (Eq. 2) (*18*, *19*).

$$3S \rightarrow \text{des}[65-72], \text{des}[40-95] \quad (2)$$

However, it was difficult by using DTT^{ox} as an oxidizing reagent to observe evolution of the stable structures coupled with these SS rearrangement steps because of the existence of excess DTT^{ox}. The problem was solved by using DHS^{ox} instead of the sulphur reagent.

As shown in Figs 6–8, gradual formation of des[65–72] and des[40–95] was clearly detected with evolution of the native-like structures. The population of N (%N) was ~18% after the reaction time of 300 min in Fig. 6, which was not enough to fully explain the UV spectral changes observed in Fig. 7 although the initial concentrations of R ($[R]_0$) in the experiments of Figs 6 and 7 were slightly different: about 60% of the native structures already formed in 300 min according to the UV spectral change. Since R, 1S, 2S, 3S and 4S intermediates do not have folded structures as discussed earlier, it is obvious that the des[65–72] and des[40–95] intermediates have native-like structures. Thus, it is unambiguously proved that stable structures suddenly form during the SS rearrangement processes from 3S to des[65–72] and des[40–95] (*45*). The exact rates of the reactions could not be determined from the chromatograms due to the

peak overlapping, but the apparent rate deducible from the observed spectral changes would be reasonable as compared with the rate constants reported previously; $k_{3S \rightarrow des[65–72]} = 0.0021\,min^{-1}$ and $k_{3S \rightarrow des[40–95]} = 0.014\,min^{-1}$ (*19*). It is also notable that according to Figs 7 and 8 the global conformational folding and the accumulation of the secondary structures occur simultaneously. The observed synchronous behaviour reasonably supports the quasi-stochastic mechanism of SS-coupled protein folding (*45*), in which the conformational folding to the stable structures does not take place unless the correct SS linkages are formed.

Final Events to Native RNase A—In careful investigation on the HPLC chromatograms shown in Fig. 6, one should notice a couple of reactions that proceed with the reaction of Eq. 2.

The first reaction is slow formation of N,

$$\text{des[65–72], des[40–95]} \xrightleftharpoons[\text{red}]{\text{ox}} \text{N} \qquad (3)$$

Since formation of N follows formation of des[65–72] and des[40–95] in the series of chromatograms, it is obvious that N is produced from these intermediates by oxidation. However, no oxidant (*i.e*. DHS^{ox}) was left in the reaction solution. Therefore, the possibility of air oxidation was suspected. To evaluate the rate of air oxidation, we carried out the same long-term folding experiments in a globe box filled with argon. The resulting HPLC charts (data not shown), however, showed no significant difference with those in Fig. 6, suggesting that air oxidation of the cysteinyl SH groups was slow at pH 8.0 and 25°C. Therefore, to explain the generation of native RNase A (N) the mechanisms other than air oxidation, such as intermolecular SH–SS exchange reactions, are to be considered.

The second reaction is the decrease of 4S, 2S, 1S and R intermediates with increasing a reaction time, which is a little unusual because only the 3S ensemble must be consumed if the rearrangement from 3S to des[65–72] and des[40–95] (Eq. 2) solely occurred. Since the SS formation reaction of Eq. 1 is already completed in 1 min and the SS cleavage reaction (*i.e*. the reverse reaction of Eq. 1) should be negligible, only intermolecular SH–SS exchange reactions (*46*), such as shown in Eq. 4, can reasonably explain the observed diminution of 4S, 2S, 1S and R.

$$\left.\begin{aligned} 1S + 4S &\rightleftarrows 2S + 3S \\ 2S + 4S &\rightleftarrows 2(3S) \end{aligned}\right\} \qquad (4)$$

These reactions must proceed very slowly in the both directions and be sensitive to the concentrations (*46*). Similar intermolecular exchange reactions have been reported in the SS-rearrangement experiment using the isolated 3S intermediate ensemble (*18*). It should be noted that in the presence of only 4S ensemble (*i.e*. in the 1 : 4 mixture of R and DHS^{ox}) formation of 3S, des[65–72] and des[40–95] was never observed in the long-term folding experiment even when an excess amount of DHS^{red} was added to the solution. If the intermolecular SH–SS exchange reaction is possible, N can be produced by using the similar mechanism.

CONCLUSIONS

Oxidative folding pathways of RNase A have been extensively studied by using various redox couples (*11–13*, *17–19*), and the reaction scheme of Fig. 2 is now accepted as the major pathways (*18*, *19*). In this article, we reinvestigated the folding pathways of RNase A by using a new selenoxide reagent (*7*, *8*), which has strong oxidation power, to demonstrate the usefulness as an oxidative folding reagent. Indeed, the folding scheme shown in Fig. 2 was successfully separated into three distinct events; the fast stochastic SS formation without generation of stable structures (Eq. 1), the slow SS rearrangement from 3S to des[65–72] and des[40–95] intermediates accompanied with generation of native-like stable structures (Eq. 2) and the final SS formation between Cys65 and Cys72 or Cys40 and Cys95 to gain the native structures (Eq. 3) via slow intermolecular SH–SS exchange reaction (Eq. 4). It is notable that the folding pathways did not change by applying DHS^{ox} as an oxidizing reagent, although the rate-limiting steps were shifted from processes *a* and *b* to processes *c* and *d* (Fig. 2). This suggests that the major oxidative folding pathways of RNase A are robust against a sort of redox couples being employed.

Advantageous features of DHS^{ox} as a potent oxidizing reagent for protein folding study can be summarized as follows. DHS^{ox} reacts with cysteinyl SH groups to produce a SS linkage rapidly and quantitatively. Therefore, SS formation and SS rearrangement reactions can be clearly separated under weakly basic conditions. This allows not only facile investigation on the conformational folding processes coupled with SS rearrangement but also clear observation of the stable key intermediates on the folding pathways, just by mixing the solutions of the reduced protein (R) and DHS^{ox}. This simple way of investigation on redox-coupled protein folding pathways would be applicable for other various proteins with several SS linkages. Another important feature of DHS^{ox} is the applicability in a wide range of pH (al least pH 3–9). The feature would also be useful for the oxidative protein folding study because the relative rate of SS formation to SS rearrangement (or SS reshuffling) can be controlled by changing the pH of the solution.

Supplementary data are available at *JB* online.

We thank H. A. Scheraga and M. Narayan for critical reading of the manuscript and valuable comments. This work was supported by Grant-in-Aid for Scientific Research (B) (No. 16350092) from the Ministry of Education, Culture, Sports, Science and Technology of Japan and Fellowships to M.I. from Sumitomo Foundation and the Association for the Progress of New Chemistry of Japan.

REFERENCES

1. Anfinsen, C.B. (1973) Principles that govern the folding of protein chains. *Science* **181**, 223–230
2. Baldwin, R.L. (1975) Intermediates in protein folding reactions and the mechanism of protein folding. *Annu. Rev. Biochem.* **44**, 453–475
3. Creighton, T.E. (1997) Protein folding coupled to disulphide bond formation. *Biol. Chem.* **378**, 731–744

4. Wedemeyer, W.J., Welker, E., Narayan, M., and Scheraga, H.A. (2000) Disulfide bonds and protein folding. *Biochemistry* **39**, 4207–4216
5. Frand, A.R., Cuozzo, J.W., and Kaiser, C.A. (2000) Pathways for protein disulfide bond formation. *Trends Cell Biol.* **10**, 203–210
6. Woycechowsky, K.J. and Raines, R.T. (2000) Native disulfide bond formation in proteins. *Curr. Opin. Chem. Biol.* **4**, 533–539
7. Iwaoka, M. and Tomoda, S. (2000) *trans*-3,4-Dihydroxy-1-selenolane oxide: a new reagent for rapid and quantitative formation of disulfide bonds in polypeptides. *Chem. Lett.* 1400–1401
8. Iwaoka, M., Takahashi, T., and Tomoda, S. (2001) Syntheses and structural characterization of water-soluble selenium reagents for the redox control of protein disulfide bonds. *Heteroatom Chem.* **12**, 293–299
9. Raines, R.T. (1998) Ribonuclease A. *Chem. Rev.* **98**, 1045–1065
10. Chatani, E. and Hayashi, R. (2001) Functional and structural roles of constituent amino acid residues of bovine pancreatic ribonuclease A. *J. Biosci. Bioeng.* **92**, 98–107
11. Narayan, M., Welker, E., Wedemeyer, W.J., and Scheraga, H.A. (2000) Oxidative folding of proteins. *Acc. Chem. Res.* **33**, 805–812
12. Rothwarf, D.M. and Scheraga, H.A. (1993) Regeneration of bovine pancreatic ribonuclease A. 1. Steady-state distribution. *Biochemistry* **32**, 2671–2679
13. Rothwarf, D.M. and Scheraga, H.A. (1993) Regeneration of bovine pancreatic ribonuclease A. 2. Kinetics of regeneration. *Biochemistry* **32**, 2680–2689
14. Creighton, T.E. and Goldenberg, D.P. (1984) Kinetic role of a meta-stable native-like two-disulfide species in the folding transition of bovine pancreatic trypsin inhibitor. *J. Mol. Biol.* **179**, 497–526
15. Creighton, T.E. (1990) Protein folding. *Biochem. J.* **270**, 1–16
16. Weissman, J.S. and Kim, P.S. (1991) Reexamination of the folding of BPTI: predominance of native intermediates. *Science* **253**, 1386–1393
17. Neira, J.L. and Rico, M. (1997) Folding studies on ribonuclease A, a model protein. *Fold Des.* **2**, R1–R11
18. Rothwarf, D.M., Li, Y.-J., and Scheraga, H.A. (1998) Regeneration of bovine pancreatic ribonuclease A: identification of two nativelike three-disulfide intermediates involved in separate pathways. *Biochemistry* **37**, 3760–3766
19. Rothwarf, D.M., Li, Y.-J., and Scheraga, H.A. (1998) Regeneration of bovine pancreatic ribonuclease A: detailed kinetic analysis of two independent folding pathways. *Biochemistry* **37**, 3767–3776
20. Anderson, W.L. and Wetlaufer, D.B. (1976) The folding pathway of reduced lysozyme. *J. Biol. Chem.* **251**, 3147–3153
21. Roux, P., Delepierre, M., Goldberg, M.E., and Chaffotte, A.-F. (1997) Kinetics of secondary structure recovery during the refolding of reduced hen egg white lysozyme. *J. Biol. Chem.* **272**, 24843–24849
22. van den Berg, B., Chung, E.W., Robinson, C.V., and Dobson, C.M. (1999) Characterization of the dominant oxidative folding intermediate of hen lysozyme. *J. Mol. Biol.* **290**, 781–796
23. van den Berg, B., Chung, E.W., Robinson, C.V., Mateo, P.L., and Dobson, C.M. (1999) The oxidative refolding of hen lysozyme and its catalysis by protein disulfide isomerase. *EMBO J.* **18**, 4794–4803
24. Jarrett, N.M., Djavadi-Ohaniance, L., Willson, R.C., Tachibana, H., and Goldberg, M.E. (2002) Immunochemical pulsed-labeling characterization of intermediates during hen lysozyme oxidative folding. *Protein Sci.* **11**, 2584–2594
25. Shioi, S., Imoto, T., and Ueda, T. (2004) Analysis of the early stage of the folding process of reduced lysozyme using all lysozyme variants containing a pair of cysteines. *Biochemistry* **43**, 5488–5493
26. Chang, C.-C., Yeh, X.-C., Lee, H.-T., Lin, P.-Y., and Kan, L.-S. (2004) Refolding of lysozyme by quasistatic and direct dilution reaction paths: a first-order-like state transition. *Phys. Rev. E* **70**, 011904
27. Chang, J.-Y. (2002) The folding pathway of α-lactalbumin elucidated by the technique of disulfide scrambling. Isolation of on-pathway and off-pathway intermediates. *J. Biol. Chem.* **277**, 120–126
28. Chang, J.-Y. and Li, L. (2002) Pathway of oxidative folding of α-lactalbumin: a model for illustrating the diversity of disulfide folding pathways. *Biochemistry* **41**, 8405–8413
29. Salamanca, S. and Chang, J.-Y. (2006) Pathway of oxidative folding of a 3-disulfide α-lactalbumin may resemble either BPTI model or hirudin model. *Protein J.* **25**, 275–287
30. Annis, I., Chen, L., and Barany, G. (1998) Novel solid-phase reagents for facile formation of intramolecular disulfide bridges in peptides under mild conditions. *J. Am. Chem. Soc.* **120**, 7226–7238
31. Shi, T. and Rabenstein, D.L. (2000) Discovery of a highly selective and efficient reagent for formation of intramolecular disulfide bonds in peptides. *J. Am. Chem. Soc.* **122**, 6809–6815
32. Shi, T. and Rabenstein, D.L. (2001) Formation of multiple intramolecular disulfide bonds in peptides using the reagent *trans*-$[Pt(ethylenediamine)_2Cl_2]^{2+}$. *Tetrahedron Lett.* **42**, 7203–7206
33. Narayan, M., Welker, E., Wanjalla, C., Xu, G., and Scheraga, H.A. (2003) Shifting the competition between the intramolecular reshuffling reaction and the direct oxidation reaction during the oxidative folding of kinetically trapped disulfide-insecure intermediates. *Biochemistry* **42**, 10783–10789
34. Lyles, M.M. and Gilbert, H.F. (1991) Catalysis of the oxidative folding of ribonuclease A by protein disulfide isomerase: dependence of the rate on the composition of the redox buffer. *Biochemistry* **30**, 613–619
35. Lyles, M.M. and Gilbert, H.F. (1991) Catalysis of the oxidative folding of ribonuclease A by protein disulfide isomerase: pre-steady-state kinetics and the utilization of the oxidizing equivalents of the isomerase. *Biochemistry* **30**, 619–625
36. Woycechowsky, K.J., Wittrup, K.D., and Raines, R.T. (1999) A small-molecule catalyst of protein folding in vitro and in vivo. *Chem. Biol.* **6**, 871–879
37. Beld, J., Woycechowsky, K.J., and Hilvert, D. (2007) Selenoglutathione: efficient oxidative protein folding by a diselenide. *Biochemistry* **46**, 5382–5390
38. Welker, E., Hathaway, L., and Scheraga, H.A. (2004) A new method for rapid characterization of the folding pathways of multidisulfide-containing proteins. *J. Am. Chem. Soc.* **126**, 3720–3721
39. Bruice, T.W. and Kenyon, G.L. (1982) Novel alkyl alkanethiolsulfonate sulfhydryl reagents. Modification of derivatives of L-cysteine. *J. Protein Chem.* **1**, 47–58
40. Xu, X., Rothwarf, D.M., and Scheraga, H.A. (1996) Nonrandom distribution of the one-disulfide intermediates in the regeneration of ribonuclease A. *Biochemistry* **35**, 6406–6417
41. Roberts, D.D., Lewis, S.D., Ballou, D.P., Olson, S.T., and Shafer, J.A. (1986) Reactivity of small thiolate anions and cysteine-25 in papain toward methyl methanethiosulfonate. *Biochemistry* **25**, 5595–5601
42. Volles, M.J., Xu, X., and Scheraga, H.A. (1999) Distribution of disulfide bonds in the two-disulfide intermediates in the regeneration of bovine pancreatic ribonuclease A: further insights into the folding process. *Biochemistry* **38**, 7284–7293
43. Hermans, J. Jr and Scheraga, H.A. (1961) Structural studies of ribonuclease. V. Reversible change of configuration. *J. Am. Chem. Soc.* **83**, 3283–3292

44. Stelea, S.D., Pancoska, P., Benight, A.S., and Keiderling, T.A. (2001) Thermal unfolding of ribonuclease A in phosphate at neutral pH: deviations from the two-state model. *Protein Sci.* **10**, 970–978
45. Welker, E., Wedemeyer, W.J., Narayan, M., and Scheraga, H.A. (2001) Coupling of conformational folding and disulfide-bond reactions in oxidative folding of proteins. *Biochemistry* **40**, 9059–9064
46. Song, M.-C. and Scheraga, H.A. (2000) Formation of native structure by intermolecular thiol-disulfide exchange reactions without oxidants in the folding of bovine pancreatic ribonuclease A. *FEBS Lett.* **471**, 177–181